

Cumulative deformation of high-speed railway bridge pier under repeated earthquakes

Hongye Gou^{*1,2}, Dan Leng^{1a}, Yi Bao^{3b} and Qianhui Pu^{1c},

¹Department of Bridge Engineering, School of Civil Engineering, Southwest Jiaotong University, Chengdu 610031, China

²Key Laboratory of High-Speed Railway Engineering, Ministry of Education, Southwest Jiaotong University, Chengdu 610031, China

³Department of Civil, Environmental and Ocean Engineering, Stevens Institute of Technology, Hoboken, NJ 07030, USA

(Received June 5, 2018, Revised February 20, 2019, Accepted February 24, 2019)

Abstract. Residual deformation of high-speed railway bridge piers is cumulative under repeated earthquakes, and influences the safety and ride comfort of high-speed trains. This paper investigates the effects of the peak ground acceleration, longitudinal reinforcement ratio, and axial compression ratio on the cumulative deformation through finite element analysis. A simply-supported beam bridge pier model is established using nonlinear beam-column elements in OpenSees, and validated against a shaking table test. Repeated earthquakes were input in the model. The results show that the cumulative deformation of the bridge piers under repeated earthquakes increases with the peak ground acceleration and the axial compression ratio, and decreases with the longitudinal reinforcement ratio.

Keywords: cumulative residual deformation; high-speed railway bridge piers; repeated earthquakes; nonlinear numerical model; parametric studies

1. Introduction

High-speed railway (HSR) represents a reliable, efficient, effective, and comfortable transportation solution for the congestion in China (Ning *et al.* 2011, Romero *et al.* 2012, Guan *et al.* 2013, Sun *et al.* 2016). Over 25,000 kilometers of HSR was already constructed in China till 2017, which included more than 9,000 kilometers in regions where the design seismic magnitude was above 7 according to GB 18306-2015 (2015). As the HSR construction is extended to western China, longer mileage of HSR is in seismically-active zone. The HSR network in China is facing the challenge of safety under earthquake.

In the HSR network in China, bridges cover more than 50% of the total mileage because bridges minimize interruption of the existing transportation lines and land occupation (Hu *et al.* 2013, Yan *et al.* 2015). Under repeated earthquake events, the bridges are subjected to residual deformation, which accumulates and endangers the safety and riding comfort of high-speed trains (Shin *et al.* 2010, Loulelis *et al.* 2012, Aldemir *et al.* 2013, Duerr *et al.* 2013, Abdelnaby and Elnashai 2015). The permanent deformation of bridge piers causes deformation in the rail track (Gou *et al.* 2018).

Cumulative deformations due to repeated earthquakes were studied through experimentation (Shrestha *et al.* 2011, Chou and Liu 2012, Araki *et al.* 2015, Loh *et al.* 2011, Vu and Li 2018, Fu *et al.* 2015, Tian *et al.* 2018, Dong *et al.* 2017) and numerical simulations (Eatherton and Hajjar 2011, Ruiz-García and Miranda 2010, Hatzigeorgiou *et al.* 2011, Noguez and Saiidi 2013, Tang *et al.* 2016, Zhang and Alam 2016, Wang and Zhu 2018, Binder and Christopoulos 2018). Fahmy *et al.* (2010) tested 13 reinforced concrete bridge columns under seismic loading to study the effects of design variables on the residual deformation, and found that the axial load ratio was the dominate factor. Karavasilis and Seo (2011) conducted parametric studies on the seismic response of highly-damped self-centering and conventional structures, and quantified the effects of viscous damping, strength ratio, and period of vibration on the peak displacement, residual deformation, and peak acceleration. The research showed that increasing the damping ratio increased the residual deformation of the structures. Psycharis *et al.* (2013) conducted Monte Carlo simulations to assess the seismic risk of a multi-drum column under synthetic ground motions, and founded that the residual deformation of column increased with the peak ground acceleration (PGA) of the ground motions. Zhang *et al.* (2017) carried out time-history response analysis to study the influences of model parameters and ground motion on the residual deformation of single degree-of-freedom (DOF) systems under 100 ground motions, respectively. The ratios of the residual deformation to the maximum deformation of the systems under different ground motions exhibited significant scatter, and the degree of scatter was associated with the stiffness ratio, natural period, relative yield load coefficient, and peak ground acceleration. While there are numerous studies on single DOF systems under single

*Corresponding author, Associate Professor

E-mail: gouhongye@swjtu.cn

^aMaster Student

E-mail: 842006596@qq.com

^bAssistant Professor

E-mail: yi.bao@stevens.edu

^cProfessor

E-mail: qhpu@vip.163.com

earthquake, there remains lack of knowledge on multi-DOF (MDOF) system under repeated earthquakes.

This study aims to investigate the influence of key parameters on the cumulative deformation of HSR bridge piers under repeated earthquakes. The influence is investigated using a simply-supported beam bridge pier model based on nonlinear beam-column element. This study is expected to provide a tool to predict the cumulative deformation, and offer insights into the design, evaluation, and maintenance of HSR bridges.

2. Cumulative deformation of bridge piers

The effects of repeated earthquakes are not considered in the current seismic codes. However, as a matter of fact, many earthquakes are composed of a main shock and a sequence of aftershocks, as indicated by a large number of ground motion records (Moustafa and Takewaki 2012, Kostinakis and Morfidis 2017, Jamnani *et al.* 2018). Thus, the HSR bridges in seismically-active regions are often subjected to repeated earthquakes. The residual deformation of bridge pier accumulates with the earthquakes that cause residual deformation. Currently, there is no formula for calculating the cumulative deformation of bridge piers.

An approach to calculate residual deformation of piers is recommended by JRA (1996), which is the first code that uses the post-earthquake residual deformation as an index for seismic design of bridges. Eq. (1) shows the formula for determining the post-earthquake residual deformation (d_r).

$$d_r = c_r (\mu_r - r) (1 - r) d_y \quad (1)$$

$$\mu_r = \frac{1}{2} \left(\frac{S_s}{gP_a} \right)^2 + \frac{1}{2} \quad (2)$$

where r is the ratio of the initial stiffness of pier section to the yield stiffness of pier section; c_r is a coefficient, which is determined by r ; μ_r is the ductility factor of pier displacement; d_y is the yield stiffness of pier; S_s is the response acceleration of pier; P_a is the lateral force of pier.

To eliminate the effect of pier height on the residual deformation, a residual deformation ratio (θ) is defined

$$\theta = \frac{\mu}{h} \quad (3)$$

where h is the height of pier.

The residual deformation ratio of bridge piers should be no more than 10‰. However, the residual deformation ratio of some bridge piers exceeded 17.5‰, as observed after the 1995 Kobe Earthquake (Cheng *et al.* 2016). According to JRA (1996) and the residual deformation ratio of bridge piers in the 1995 Kobe Earthquake, the earthquake events N_{10} and $N_{17.5}$, when the residual deformation ratios of the piers are 10‰ and 17.5‰, are used to evaluate the cumulative deformation in this study.

3. Finite element model

3.1 Description of the bridge pier

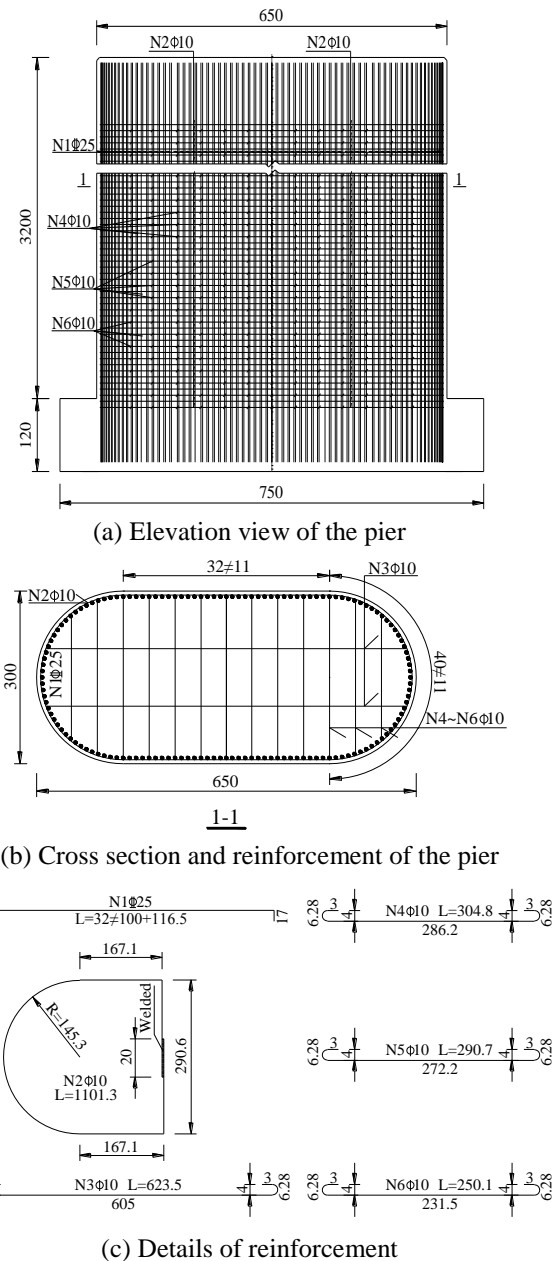


Fig. 1 Details of the high-speed railway simple supported beam bridge pier (unit: cm).

The piers of a HSR bridge in the Beijing-Shenyang Railway Line are investigated. Fig. 1 shows a 32-m, round-ended bridge pier. The cross section is 650 cm in length and 300 cm in breadth. The concrete is C35 (TB 10002.1-2005); the longitudinal reinforcing bars and stirrups are HRB400 and HPB300, respectively (GB 50010-2010). The diameter of the longitudinal bars and stirrups are 25 mm and 10 mm, respectively. Compared with normal bridge piers, the size of the HSR bridge piers is larger, and the longitudinal reinforcement ratio of the HSR bridge pier is lower. In addition, the longitudinal and transverse stiffness of the HSR bridge piers are greater to ensure adequate riding comfort of the high-speed trains.

3.2 Modeling of the high-speed railway bridge pier

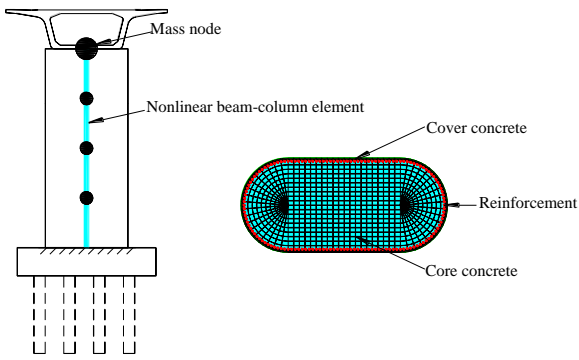
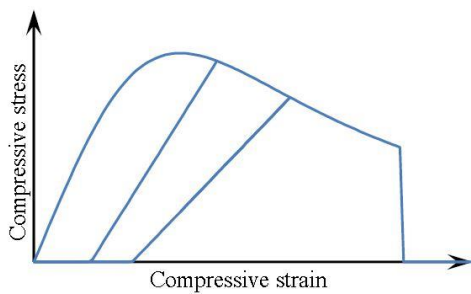
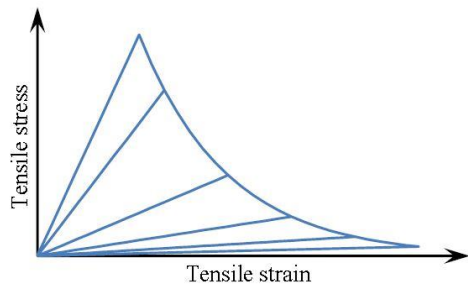


Fig. 2 The simply-supported beam bridge pier model



(a) Compressive stress-strain relationship



(b) Tensile stress-strain relationship

Fig. 3 Stress-strain relationship of Concrete04

The bridge pier is modeled using four nonlinear beam-column elements in OpenSees. The cross section of each beam-column element consists of concrete fibers and steel bar fibers, as shown in Fig. 2. For the high-speed railway bridge pier in good geological conditions, pile-soil interaction has negligible effect on the residual deformation, as elaborated in (Chen *et al.* 2011). In this study, since possible effect of the geological condition is not considered, the pile-soil interaction is not considered. The mass of the pier is equally distributed to the two nodes of each element. An additional lumped mass is applied to the top node of the pier to consider the influence of the superstructure.

The concrete fibers are simulated using Concrete04 that considers concrete stiffness degeneration. The compressive and tensile stress-strain relationships of Concrete04 are shown in Figs. 3(a) and 3(b), respectively. The compressive stress-strain relationship is based on the Sandor Popovics' model (Popovics 1973), and its stiffness degeneration during unloading and reloading is based on the Karsan-Jirsa model (Karsan and Jirsa 1969); the tensile stress-strain relationship is an exponential function, and its unloading and reloading paths are defined by the secant stiffness.

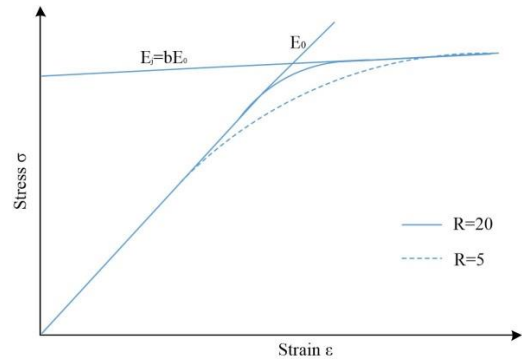
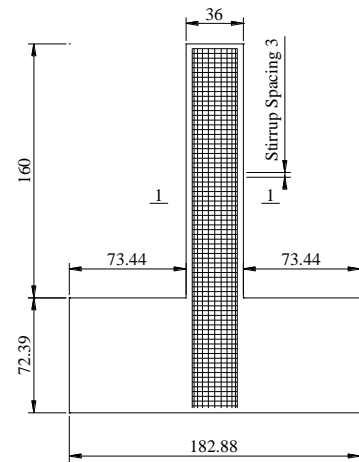
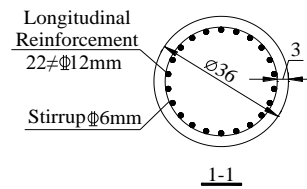


Fig. 4 Stress-strain relationship of Steel02



(a) Overall dimensions of the reinforced concrete pier



(b) Cross section and reinforcement of the pier

Fig. 5 Details of the reinforced concrete pier (unit: cm)

The steel bar fibers are simulated using Steel02, based on the Giuffre-Menegotto-Pinto model (Han *et al.* 2010). Steel02 considers the Bauschinger effect (Shafaei *et al.* 2014). The stress-strain relationship of Steel02 is shown in Fig. 4, where E_0 is the elastic modulus; b is the hardening coefficient of the reinforcing steel; R is an adjustment coefficient for the curvature of the transition curve.

3.3 Validation of the model

Model test and in-situ test are effective approaches to investigate the mechanical performance of bridges (Gou *et al.* 2018 a, b, c, d, f). In this study, a cantilever reinforced concrete pier tested by Choi *et al.* (2010) in the Large-Scale Structures Laboratory in the University of Nevada-Reno (UNR) is used to validate the finite element model.

The tested pier was flexure dominated. The details of the cantilevered reinforced concrete pier are shown in Fig. 5. The height of the pier was 1.6 m. The diameter of the cross was 0.36 m. The longitudinal reinforcement ratio was

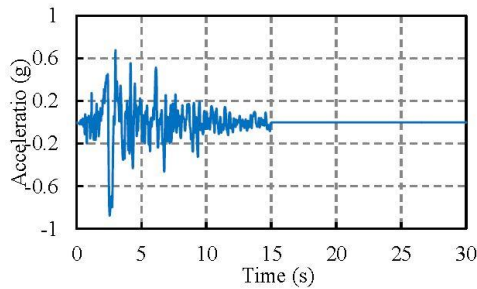


Fig. 6 Seismic waveform

2.9%; the stirrup ratio was 1.37%. The yield strength of the reinforcing bars was 490 MPa; the concrete compressive strength was 44 MPa.

The footing of the pier was anchored to a shake table. A mass rig system that was connected to the top of the pier was used to apply inertial force under seismic loading. The total equivalent weight of the inertial mass of the pier was 276 kN. The axial force was applied using a hydraulic jack and prestressed tendons, and the compression ratio was 0.08 (Choi *et al.* 2010). Residual displacements of the pier were measured.

The pier was subjected to a ground motion recorded by the Rinaldi Station in the Northridge Earthquake in 1994, as shown in Fig. 6. The seismic has a peak ground acceleration of 0.838 g, a peak ground velocity of 1.66 m/s, and a peak ground displacement of 289 mm (Pacific Earthquake Engineering Research Center 2007). To obtain the residual deformation, free vibration for 15 s was added. A total of 12 shaking table tests were carried out under ground motions with the same waveforms but different PGAs (0, 0.04, 0.08, 0.17, 0.25, 0.38, 0.50, 0.63, 0.75, 0.88, 1.01, and 1.13).

Visible cracks began to appear in the tested pier after the third test. During the fourth test, some longitudinal bar yielded. Then several flexural cracks occurred during the fifth test and extended during subsequent tests. The cover concrete of the pier base started to spall during the seventh test. During the eighth test, the spiral bar yielded, but the core concrete was not damaged. After the ninth test, the pier exhibited permanent displacement. The core concrete of the pier was obviously damaged after the eleventh test. During the twelfth test, one longitudinal bar ruptured, and several other longitudinal bars buckled (Choi *et al.* 2010).

The pier model consists of five nonlinear beam-column elements. A zero-length element is established at the bottom of the cantilevered reinforced concrete pier model using the Bond_SP01 to simulate the slip of reinforcing bar. The cover concrete fibers are simulated using Concrete01. Considering the confinement of stirrup, the core concrete fibers are simulated using Concrete02. The reinforcing bar fibers are simulated using Steel02. In the above seismic load cases, the curve and values of residual deformation are obtained and compared with test results, as shown in Fig. 7. The test and simulation results of the residual deformation agree well, indicating the finite element model provides reasonable prediction of the residual deformation.

4. Seismic input

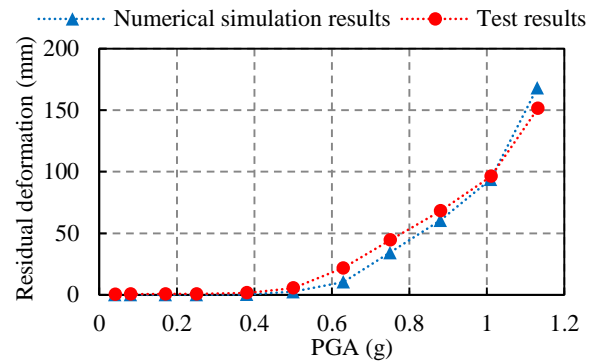
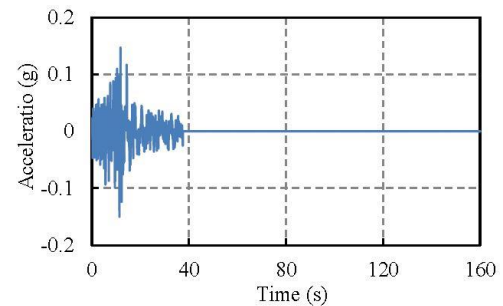
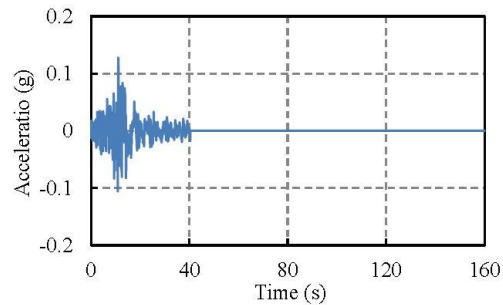


Fig. 7 Comparison of the residual deformation results



(a) X direction



(b) Y direction

Fig. 8 Chi-Chi_CHY101_1244 seismic waveform

The 1999 Chi-Chi Earthquake with a main shock of 7.6 magnitude had four strong aftershocks, which occurred within 7 days after the main shock and had magnitudes above 6.5. A seismic wave recorded by the CHY101 Station is selected to construct repeated earthquake sequences. Since this study aims to investigate the influence of the PGA, the longitudinal reinforcement ratio, and the axial compression ratio on the cumulative deformation of HSR bridge piers under repeated earthquakes, the intensity and duration of each earthquake are assumed to be the same. Parametric studies were conducted using the constructed repeated earthquake sequences as the input seismic loads, as shown in Fig. 8. To obtain the residual deformation after the vibration of the pier fully decayed, there was a time interval of $3t$ (t was the duration of last ground motion) between two seismic waves.

5. Parametric studies

5.1 Effect of the peak ground acceleration

Table 1 Residual deformation ratio of pier under different peak ground accelerations

Earthquake events	PGA=0.125 g		PGA=0.15 g		PGA=0.175 g	
	X direction	Y direction	X direction	Y direction	X direction	Y direction
1	-0.350‰	0.141‰	-0.082‰	0.008‰	-0.028‰	-0.064‰
2	-0.159‰	0.075‰	-0.098‰	0.039‰	0.195‰	-0.141‰
3	-0.207‰	0.092‰	-0.224‰	0.108‰	0.489‰	-0.950‰
4	-0.256‰	0.114‰	-0.412‰	0.233‰	3.540‰	-9.846‰
5	-0.298‰	0.135‰	-0.785‰	0.496‰	19.163‰	-27.359‰
6	-0.340‰	0.156‰	-1.560‰	1.191‰	—	—
7	-0.370‰	0.171‰	-3.003‰	3.091‰	—	—
8	-0.402‰	0.188‰	-5.105‰	7.365‰	—	—
9	-0.430‰	0.204‰	-6.815‰	13.879‰	—	—
10	-0.461‰	0.221‰	-8.157‰	28.359‰	—	—
12	-0.517‰	0.253‰	—	—	—	—
14	-0.585‰	0.292‰	—	—	—	—
16	-0.672‰	0.344‰	—	—	—	—
18	-0.781‰	0.410‰	—	—	—	—
20	-0.890‰	0.487‰	—	—	—	—
22	-1.114‰	0.640‰	—	—	—	—
24	-1.460‰	0.901‰	—	—	—	—
26	-2.032‰	1.382‰	—	—	—	—
28	-2.907‰	2.284‰	—	—	—	—
30	-4.164‰	4.241‰	—	—	—	—
32	-4.907‰	6.684‰	—	—	—	—
33	-6.423‰	9.012‰	—	—	—	—
34	-10.38‰	14.449‰	—	—	—	—
35	-19.31‰	24.152‰	—	—	—	—

Note: Negative sign in the table indicates the direction.

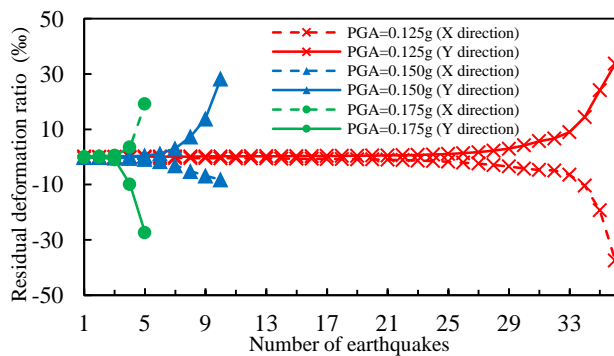


Fig. 9 Influence of PGA on the residual deformation ratio

Three PGA values (0.125 g, 0.15 g, and 0.175 g) are investigated. Fig. 9 and Table 1 show the relationship between the PGA and residual deformation ratio. As the PGA increases, the cumulative deformation and residual deformation ratio rise with increasing rates. The reason is that as a higher PGA is applied, the pier is subjected larger forces. Thus, higher inelasticity in the materials is caused, resulting in higher stiffness degradation (Abdelnaby and Elnashai 2015). Damage is accumulated with the increase of the number of earthquakes, and the residual deformation ratio increases. When the residual deformation ratio is less than 1‰, the cumulative rate of residual deformation is slow. When the residual deformation ratio is more than 2‰, the cumulative rate of residual deformation is fast. The reason is that the reinforcement in the pier is yielded as the

residual deformation ratio exceeds 2‰ (Zhou *et al.* 2014).

5.2 Effect of the longitudinal reinforcement ratio

The longitudinal reinforcement plays an important role in the earthquake resistance of bridge piers. On one hand, the longitudinal reinforcement and stirrup constrain the core concrete, increasing the strength of core concrete. On the other hand, the pier is subjected to tension and compression. Due to the weak tensile strength of concrete, the longitudinal reinforcement provides tensile strength for the pier. Moreover, the longitudinal reinforcement ratio of pier is no less than 0.5% (GB50111-2006 2006). Therefore, four HSR bridge piers with different longitudinal reinforcement ratios (0.53%, 0.64%, 0.83%, and 1.04%) are analyzed in this section.

Table 2 shows the residual deformation ratios of piers under different longitudinal reinforcement ratios. When the longitudinal reinforcement ratio is 0.53%, the residual deformation ratio (Y direction) is -4.405‰ after 4 earthquakes, and -36.89‰ after 5 earthquakes. However, when the longitudinal reinforcement ratio of pier is 1.04%, the residual deformation ratio of pier (Y direction) is 7.465‰ after fifteen earthquakes and is 10.139‰ after 14 earthquakes. Therefore, the cumulative rates of residual deformation under different longitudinal reinforcement ratios are different. A higher longitudinal reinforcement ratio improves the ductility and the capability of resisting cumulative deformation, and reduce the cumulative rate of

Table 2 Residual deformation ratio of pier under different longitudinal reinforcement ratios

Earthquake events	$\rho=0.53\%$		$\rho=0.64\%$		$\rho=0.83\%$		$\rho=1.04\%$	
	X direction	Y direction						
1	0.037‰	-0.041‰	0.006‰	-0.020‰	-0.082‰	0.008‰	-0.275‰	0.067‰
2	0.093‰	-0.075‰	0.057‰	-0.038‰	-0.098‰	0.039‰	-0.372‰	0.065‰
3	0.252‰	-0.283‰	0.110‰	-0.063‰	-0.224‰	0.108‰	-0.541‰	0.135‰
4	1.508‰	-4.405‰	0.206‰	-0.135‰	-0.412‰	0.233‰	-0.673‰	0.191‰
5	27.518‰	-36.89‰	0.384‰	-0.412‰	-0.785‰	0.496‰	-0.814‰	0.271‰
6	—	—	0.716‰	-4.359‰	-1.560‰	1.191‰	-0.982‰	0.377‰
7	—	—	6.651‰	-21.53‰	-3.003‰	3.091‰	-1.207‰	0.535‰
8	—	—	39.628‰	-49.12‰	-5.105‰	7.365‰	-1.544‰	0.779‰
9	—	—	—	—	-6.815‰	13.879‰	-1.985‰	1.137‰
10	—	—	—	—	-8.157‰	28.359‰	-2.476‰	1.590‰
11	—	—	—	—	—	—	-3.041‰	2.208‰
12	—	—	—	—	—	—	-3.696‰	3.073‰
13	—	—	—	—	—	—	-4.352‰	4.190‰
14	—	—	—	—	—	—	-5.113‰	5.697‰
15	—	—	—	—	—	—	-6.014‰	7.465‰
16	—	—	—	—	—	—	-8.123‰	10.139‰
17	—	—	—	—	—	—	-13.214‰	15.879‰
18	—	—	—	—	—	—	-24.243‰	22.726‰
19	—	—	—	—	—	—	-42.842‰	25.744‰
20	—	—	—	—	—	—	-70.451‰	27.344‰

Note: Negative sign in the table indicates the direction.

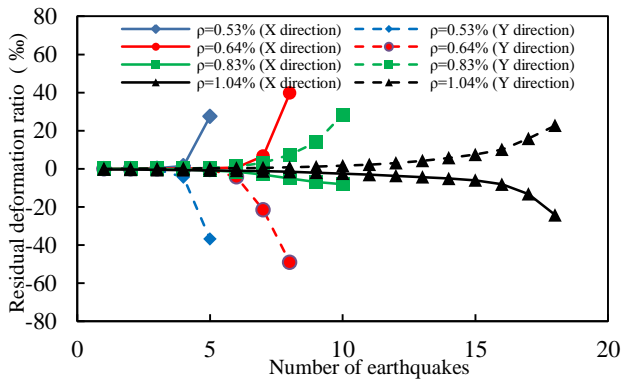


Fig. 10 Influence of longitudinal reinforcement ratio on residual deformation ratio

residual deformation. Besides, the residual deformation ratio increases with the number of earthquakes.

The relationship between the longitudinal reinforcement ratio and the residual deformation ratio of pier are shown in Fig. 10. It can be seen that the residual deformation ratio of pier with lower longitudinal reinforcement ratio suddenly increases after several earthquakes. The residual deformation ratio of pier with higher longitudinal reinforcement ratio also increases nonlinearly with earthquake events; however the increasing rate is slower than that of pier with lower longitudinal reinforcement ratio. The reason is that the reinforcing steel provides the plastic deformation capacity for pier during earthquakes. For pier with lower longitudinal reinforcement ratio, the stiffness degeneration is serious after several earthquakes, then the residual deformation increases sharply, and pier may be destroyed suddenly because of too large residual

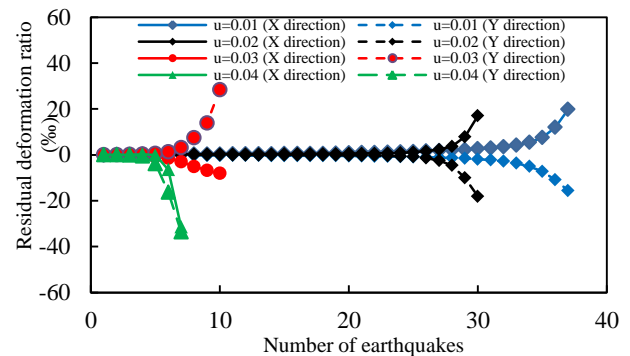


Fig. 11 Influence of axial compression ratio on residual deformation ratio of pier

deformation. However, for pier with higher longitudinal reinforcement ratio, the deformation capacity that the reinforcing steel provides is stronger, the residual deformation increases slowly, and plastic failure occurs.

5.3 Effect of the axial compression ratio

To ensure adequate capabilities of plastic deformation capacity and collapse resistance capacity of pier, the largest axial compression ratio is stipulated in GB50011-2010 (2010) and GB50010-2010 (2010). In this section, 4 high-speed railway bridge piers under different axial compression ratios (0.01, 0.02, 0.03, and 0.04) were utilized to analyze the effect of the axial compression ratio on the cumulative residual deformation.

Table 3 and Fig. 11 display the change of the residual deformation ratio of piers under different axial compression ratios. The cumulative rate of the residual deformation

Table 3 Residual deformation ratio of pier under different axial compression ratios

Number of earthquake	$u=0.04$		$u=0.03$		Number of earthquake	$u=0.02$		$u=0.01$	
	X direction	Y direction	X direction	Y direction		X direction	Y direction	X direction	Y direction
1	-0.050‰	0.035‰	-0.082‰	0.008‰	1	-0.182‰	0.041‰	-0.094‰	-0.124‰
2	-0.018‰	-0.011‰	-0.098‰	0.039‰	4	0.163‰	-0.020‰	0.229‰	-0.195‰
3	0.065‰	-0.117‰	-0.224‰	0.108‰	7	0.239‰	-0.044‰	0.284‰	-0.230‰
4	0.232‰	-0.515‰	-0.412‰	0.233‰	10	0.294‰	-0.066‰	0.346‰	-0.271‰
5	-0.107‰	-3.883‰	-0.785‰	0.496‰	13	0.336‰	-0.092‰	0.443‰	-0.332‰
6	-6.440‰	-16.280‰	-1.560‰	1.191‰	16	0.391‰	-0.126‰	0.534‰	-0.401‰
7	-31.410‰	-33.600‰	-3.003‰	3.091‰	19	0.476‰	-0.186‰	0.685‰	-0.472‰
8	—	—	-5.105‰	7.365‰	22	0.618‰	-0.329‰	1.048‰	-0.681‰
9	—	—	-6.815‰	13.879‰	25	1.144‰	-0.898‰	1.447‰	-0.932‰
10	—	—	-8.157‰	28.359‰	28	3.656‰	-4.646‰	2.057‰	-1.398‰
29	—	—	—	—	29	7.833‰	-10.069‰	2.287‰	-1.584‰
30	—	—	—	—	30	16.993‰	-18.096‰	2.625‰	-1.887‰
31	—	—	—	—	31	—	—	3.002‰	-2.266‰
34	—	—	—	—	34	—	—	5.396‰	-5.037‰
35	—	—	—	—	35	—	—	7.487‰	-7.232‰
36	—	—	—	—	36	—	—	11.936‰	-10.921‰
37	—	—	—	—	37	—	—	19.761‰	-15.607‰

Note: Negative sign in the table indicates the direction.

increases with the axial compression ratio. When the axial compression ratio is 0.01, the residual deformation ratio of pier (Y direction) is -7.232‰ after 35 earthquakes. When the axial compression ratio of pier is 0.04, the residual deformation ratio of pier (Y direction) is -16.28‰ after 6 earthquakes. The reason is that a smaller axial compression ratio improves the initial lateral stiffness of pier. With the influence of $P-\Delta$ effect, the lateral resisting capability of the pier is enhanced. Therefore, the lateral displacement of pier under the larger axial compression ratio is amplified under the same earthquake. The increasing rate of residual deformation ratio increases with the axial compression ratio. In addition, the residual deformation ratio also increases with the number of earthquake.

5.4 Suggestions for controlling residual deformation

According to the above parametric studies, the following suggestions are proposed for controlling the residual deformation:

- The cumulative deformation of pier increases nonlinearly with the increase of the PGA. Therefore, when designing the pier in seismically-active zones, it should be conservatively assumed that the earthquake with larger magnitude occurs firstly, and then the earthquake with smaller magnitude follows.
- With the increase of longitudinal reinforcement ratio, the cumulative deformation of pier decreases under the same earthquake events. Therefore, the longitudinal reinforcement ratio of pier can be increased properly to improve the ductility of pier and strengthen the plastic deformation capacity of pier.
- The cumulative deformation of pier increases with the axial compression ratio of pier. In order to decrease the cumulative deformation of pier under repeated earthquakes, the axial compression ratio of pier has to be decreased.

According to the definition of axial compression ratio, there are two ways to decrease the axial compression ratio of pier. On the one hand, the weight of bridge superstructure can be decreased. On the other hand, the bearing capacity of pier can be increased, such as increasing the cross section of pier, improving the concrete compressive strength and increasing the number or the diameter of longitudinal reinforcement.

- Real-time bridge health monitoring in seismically active zones is suggested for HSR bridges in seismically active areas. In view of the adverse effect of the nonrenewable, long-standing and sustainable cumulative deformation of pier on the track regularity, the rail deformation should be evaluated and controlled to ensure safe operation of HSR bridges.

6. Conclusions

Based on the above investigation, the following conclusions can be drawn:

- The cumulative deformation of high-speed railway bridge pier under repeated earthquakes is nonlinearly related to the peak ground acceleration. Increasing the peak ground acceleration increases the damage caused by seismic load and the cumulative deformation.
- As the longitudinal reinforcement ratio of pier rises, the resistance to the cumulative deformation increases, and the accumulation rate of residual deformation decreases.
- The accumulation rate of residual deformation increases with the axial compression ratio. Increasing the axial compression ratio increases the initial lateral stiffness of bridge pier and the cumulative residual deformation, which has adverse effects on running safety of high-speed railway.

Acknowledgments

The research was funded by the National Natural Science Foundation of China (Grant Number 51878563), the Sichuan Science and Technology Program (Grant Numbers. 2018JY0294 and 2018JY0549), and the Science and Technology Research and Development Plan of China Railway Construction (Grant No. 2014-C34).

Reference

- Abdelnaby, A.E. and Elnashai, A.S. (2015), "Numerical modeling and analysis of RC frames subjected to multiple earthquakes", *Earthq. Struct.*, **9**(5), 957-981.
- Aldemir, A., Erberik, M.A., Demirel, I.O. and Sucuoğlu, H. (2013), "Seismic performance assessment of unreinforced masonry buildings with a hybrid modeling approach", *Earthq. Spectra*, **29**(1), 33-57.
- Araki, Y., Shrestha, K.C., Maekawa, N., Koetaka, Y., Otori, T. and Kainuma, R. (2016), "Shaking table tests of steel frame with superelastic Cu-Al-Mn SMA tension braces", *Earthq. Eng. Struct.*, **45**(2), 297-314.
- Binder, J. and Christopoulos, C. (2018), "Seismic performance of hybrid ductile-rocking braced frame system", *Earthq. Eng. Struct.*, **47**(6), 1394-1415.
- Chen, L.K., Jiang, L.Z., Yu, Z.W. and Luo, B.F. (2011), "Seismic response characteristics of a high-speed railway simply supported girder bridge", *Earthq. Eng. Eng. Vib.*, **30**(12), 216-222.
- Cheng, H., Li, H.N., Wang, D.S., Sun, Z.G., Li, G.Q. and Jin, J.N. (2016), "Research on the influencing factors for residual displacements of RC bridge columns subjected to earthquake loading", *B. Earthq. Eng.*, **14**(8), 2229-2257.
- Choi, H., Saiidi, M.S., Somerville, P. and Elazazy, S. (2010), "Experimental study of reinforced concrete bridge columns subjected to near-fault ground motions", *Aci Struct. J.*, **107**(1), 3-12.
- Chou, C.C. and Liu, J.H. (2012), "Frame and brace action forces on steel corner gusset plate connections in buckling-restrained braced frames", *Earthq. Spectra*, **28**(2), 531-551.
- Dong, H.H., Du, X.L., Han, Q., Hao, H., Bi, K.M. and Wang, X.Q. (2017), "Performance of an innovative self-centering buckling restrained brace for mitigating seismic responses of bridge structures with double-column piers", *Eng. Struct.*, **148**, 47-62.
- Duerr, K., Tesfamariam, S., Wickramasinghe, V. and Grewal, A. (2013), "Variable stiffness smart structure systems to mitigate seismic induced building damages", *Earthq. Eng. Struct.*, **42**(2), 221-237.
- Eatherton, M.R. and Hajjar, J.F. (2011), "Residual drifts of self-centering systems including effects of ambient building resistance", *Earthq. Spectra*, **27**(3), 719-744.
- Fahmy, M.F.M., Wu, Z.S., Wu, G. and Sun, Z.Y. (2010), "Post-yield stiffnesses and residual deformations of RC bridge columns reinforced with ordinary rebars and steel fiber composite bars", *Eng. Struct.*, **32**(9), 2969-2983.
- Fu, J.P., Wu, Y.T. and Yang, Y.B. (2015), "Effect of reinforcement strength on seismic behavior of concrete moment frames", *Earthq. Struct.*, **9**(4), 699-718.
- GB 18306-2015 (2015), Seismic Ground Motion Parameters Zonation Map of China, Standardization Administration of the People's Republic of China, Beijing, China.
- GB 50010-2010 (2010), Code for Design of Concrete Structures, Ministry of Housing and Urban-Rural Construction of the People's Republic of China, Beijing, China.
- GB 50011-2010 (2010), Code for Seismic Design of Buildings, Ministry of Construction of the People's Republic of China, Beijing, China.
- Gou, H.Y., He, Y.N., Zhou, W., Bao, Y. and Chen, G.D. (2018a), "Experimental and numerical investigations of the dynamic responses of an asymmetrical arch railway bridge", *P. I. Mech. Eng. F-J. RAI*, **232**(9), 2309-2323.
- Gou, H.Y., Long, H., Bao, Y., Chen, G.D., Pu, Q.H. and Kang, R. (2018b), "Experimental and numerical studies on stress distributions in girder-arch-pier connections of long-span continuous rigid frame arch railway bridge", *J. Bridge Eng.*, **23**(7), 04018039.
- Gou, H.Y., Shi, X.Y., Zhou, W., Cui, K. and Pu, Q.H. (2018c), "Dynamic performance of continuous railway bridges: Numerical analyses and field tests", *P. I. Mech. Eng. F-J RAI*, **232**(3), 936-955.
- Gou, H.Y., Wang, W., Shi, X.Y., Pu, Q.H. and Kang, R. (2018d), "Behavior of steel-concrete composite cable anchorage system", *Steel Compos. Struct.*, **26**(1), 115-123.
- Gou, H.Y., Yang, L.C., Leng, D., Bao, Y. and Pu, Q.H. (2018), "Effect of bridge lateral deformation on track geometry of high-speed railway", *Steel Compos. Struct.*, **29**(2), 219-229.
- Gou, H.Y., Zhou, W., Bao, Y., Li, X.B. and Pu, Q.H. (2018f), "Experimental study on dynamic effects of a long-span railway continuous beam bridge", *Appl. Sci.*, **8**(5), 669.
- Gou, H.Y., Zhou, W., Chen, G.D., Bao, Y. and Pu, Q.H. (2018e), "In-situ test and dynamic analysis of a double-deck tied-arch bridge", *Steel Compos. Struct.*, **27**(1), 161-175.
- Guan, K., Zhong, Z.D., Ai, B. and Kürner, T. (2013), "Deterministic propagation modeling for the realistic high-speed railway environment", *J. Mol. Biol.*, **14**(2382), 1-5.
- Han, Z.F., Ye, A.J. and Fan, L.C. (2010), "Effects of riverbed scour on seismic performance of high-rise pile cap foundation", *Earthq. Eng. Eng. Vib.*, **9**(4), 533-543.
- Hatzigeorgiou, G.D., Papagiannopoulos, G.A. and Beskos, D.E. (2011), "Evaluation of maximum seismic displacements of SDOF systems from their residual deformation", *Eng. Struct.*, **33**(12), 3422-3431.
- Hu, S.T., Niu, B., Ke, Z.T. and Liu, X.G. (2013), "Study on the optimization of standard span length simply supported box girder for high-speed railway", *China Railw. Sci.*, **34**(1), 15-21.
- Jamnani, H.H., Amiri, J.V. and Rajabnejad, H. (2018), "Energy distribution in RC shear wall-frame structures subject to repeated earthquakes", *Soil Dyn. Earthq. Eng.*, **107**, 116-128.
- JRA (Japan Road Association) (1996), Design Specification of Highway Bridges Part V. Seismic Design, Japan Road Association (JRA), Tokyo, Japan.
- Karavasilis, T.L. and Seo, C.Y. (2011), "Seismic structural and non-structural performance evaluation of highly damped self-centering and conventional systems", *Eng. Struct.*, **33**(8), 2248-2258.
- Karsan, I.D. and Jirsa, J.O. (1969), "Behavior of concrete under compressive loading", *J. Struct. Div.*, **95**(12), 2543-2564.
- Kostinakis, K. and Morfidis, K. (2017), "The impact of successive earthquakes on the seismic damage of multistorey 3D R/C buildings", *Earthq. Struct.*, **12**(1), 1-12.
- Loh, C.H., Mao, C.H., Huang, J.R. and Pan, T.C. (2011), "System identification of degrading hysteresis of reinforced concrete frames", *Earthq. Eng. Struct.*, **40**(6), 623-640.
- Loulelis, D., Hatzigeorgiou, G.D. and Beskos, D.E. (2012), "Moment resisting steel frames under repeated earthquakes", *Earthq. Struct.*, **3**(3-4), 231-248.
- Moustafa, A. and Takewaki, I. (2012), "Characterization of earthquake ground motion of multiple sequences", *Earthq. Struct.*, **3**(5), 629-647.
- Ning, B., Tang, T., Dong, H.R., Wen, D., Liu, D.R., Gao, S.G. and Wang, J. (2011), "An introduction to parallel control and management for high-speed railway systems", *IEEE T. Intell.*

- Tran.*, **12**(4), 1473-1483.
- Noguez, C.A.C. and Saiidi, M.S. (2013), "Performance of advanced materials during earthquake loading tests of a bridge system", *J. Struct. Eng.*, ASCE, **139**(1), 144-154.
- Popovics, S. (1973), "A numerical approach to the complete stress-strain curve of concrete", *Cement Concrete Res.*, **3**(5), 583-599.
- Psycharis, I.N., Fragiadakis, M. and Stefanou, I. (2013), "Seismic reliability assessment of classical columns subjected to near source ground motions", *Earthq. Eng. Struct.*, **42**(14), 2061-2079.
- Romero, A., Galvin, P. and Dominguez, J. (2012), "A time domain analysis of train induced vibrations", *Earthq. Struct.*, **3**(3), 297-313.
- Ruiz-García, J. and Miranda, E. (2010), "Probabilistic estimation of residual drift demands for seismic assessment of multi-story framed buildings", *Eng. Struct.*, **32**(1), 11-20.
- Shafaei, J., Zareian, M.S., Hosseini, A. and Marefat, M.S. (2014), "Effects of Joint Flexibility on Lateral Response of Reinforced Concrete Frames", *Eng. Struct.*, **81**(15), 412-431.
- Shin, J.U., Lee, K.H., Lee, D.H. and Jeong, S.H. (2010), "Seismic behavior of a five-story RC structure retrofitted with buckling-restrained braces using time-dependent elements", *J. Virol.*, **14**(6), 830-833.
- Shrestha, K.C., Araki, Y., Nagae, T., Omori, T., Sutou, Y., Kainuma, R. and Ishida, K. (2011), "Applicability of Cu-Al-Mn shape memory alloy bars to retrofitting of historical masonry constructions", *Earthq. Struct.*, **2**(3), 233-256.
- Sun, L.M., Xie, W.P., He, X.W. and Hayashikawa, T. (2016), "Prediction and mitigation analysis of ground vibration caused by running high-speed trains on rigid-frame viaducts", *Earthq. Eng. Eng. Vib.*, **15**(1), 31-47.
- Tang, Z.Z., Xie, X. and Wang, T. (2016), "Residual seismic performance of steel bridges under earthquake sequence", *Earthq. Struct.*, **11**(4), 649-664.
- TB 10002.1-2005 (2005), Fundamental Code for Design on Railway Bridge and Culvert, Ministry of Railways of the People's Republic of China, Beijing, China.
- Tian, X.H., Su, M.Z., Lian, M., Wang, F. and Li, S. (2018), "Seismic behavior of k-shaped eccentrically braced frames with high-strength steel: shaking table testing and fem analysis", *J. Constr. Steel Res.*, **143**, 250-263.
- Vu, N.S. and Li, B. (2018), "Seismic performance assessment of corroded reinforced concrete short columns", *J. Struct. Eng.*, ASCE, **144**(4), 04018018.
- Wang, B. and Zhu, S.Y. (2018), "Seismic behavior of self-centering reinforced concrete wall enabled by superelastic shape memory alloy bars", *B. Earthq. Eng.*, **16**(1), 479-502.
- Yan, B., Dai, G.L. and Hu, N. (2015), "Recent development of design and construction of short span high-speed railway bridges in China", *Eng. Struct.*, **100**(1), 707-717.
- Zhang, Q. and Alam, M.S. (2016), "Evaluating the seismic behavior of segmental unbounded posttensioned concrete bridge piers using factorial analysis", *J. Bridge Eng.*, **21**(4), 04015073.
- Zhang, Q., Gong, J.X. and Zhou, J.K. (2017), "Seismic residual deformation analysis of single degree of freedom system based on probability", *J. Build. Struct.*, **38**(8), 74-82.
- Zhou, D.C., Dong, Z.C., Shao, J.H. and Wang, L. (2014), "Study on displacement ductility performance of RC highway bridge columns", *Earthq. Eng. Eng. Vib.*, **1**(3), 62-67.